

## DEHYDRATION STUDIES OF Co(II), Cu(II) AND Zn(II) METHANESULFONATES

M. Wang<sup>1</sup>, H. Jiang<sup>2\*</sup> and Z. C. Wang<sup>1</sup>

<sup>1</sup>Department of Chemistry, School of Sciences, Northeastern University, Shenyang 110004, P.R. China

<sup>2</sup>Liaoning University of Petroleum and Chemical Technology, Fushun 113001, P.R. China

The dehydration process of Co(II), Cu(II) and Zn(II) methanesulfonates was studied by thermogravimetry/derivative thermogravimetry (TG/DTG) and differential scanning calorimetry (DSC) techniques in dynamic N<sub>2</sub> atmosphere. The TG/DTG curves show that all of them contain four crystallization water molecules, which are lost in two steps. The peak temperature and dehydration enthalpies  $\Delta H$  were measured from DSC curves for each compound. The effect of procedural variables on the TG and DSC curves was investigated. In this work, the procedural variables included heating rate, Al pan state (unsealed and sealed) and sample mass.

**Keywords:** dehydration, DSC, FTIR, methanesulfonates, TG/DTG

### Introduction

Metallic salts of sulfonic acid have been extensively investigated because of their excellent catalytic activity in organic reactions such as Aldol and Diels–Alder reactions [1], Biginelli reaction [2], esterification [3] and acylation [4], etc. The works that have been published are mainly concerned with the structure [5–7] and the thermal decomposition behavior of them [8–11]. There are few data relating to the dehydration [12, 13], especially for transition metal methanesulfonates.

In the present paper we report the dehydration process of Co(II), Cu(II) and Zn(II) tetrahydrated methanesulfonates in N<sub>2</sub> atmosphere using TG/DTG and DSC measurements. The effect of different heating rates, Al pan state (unsealed and sealed) and sample mass on the dehydration process has been studied in detail.

### Experimental

#### Sample preparation

The methanesulfonates were prepared in aqueous solution by heating methanesulfonic acid (analytical grade, >99.0%) and excess metal oxide or carbonate. The solutions obtained were concentrated, filtered and allowed to crystallize in air at room temperature. The products were purified by successive recrystallizations. Elemental analysis, complexometric titration, XRD and thermal analysis techniques are used for characterization of the methanesulfonates. The analytic results are in good agreement with literature [9]. It can be concluded that stoichiometric formula of the compounds is  $M(\text{CH}_3\text{SO}_3)_2 \cdot 4\text{H}_2\text{O}$  ( $M=\text{Co}$ , Cu and Zn) by above experiments.

#### Physical measurements

Infrared spectra were recorded on Perkin-Elmer Spectrum GX with resolution of  $4\text{ cm}^{-1}$  in the wave number range  $4000\text{--}600\text{ cm}^{-1}$ . TG curves were monitored on a Perkin-Elmer Pyris 1 TGA (sample mass is about 2.5 mg). Experiments were conducted in dynamic N<sub>2</sub> atmosphere ( $20\text{ mL min}^{-1}$ ) at a heating rate of 5, 10, 15,  $20^\circ\text{C min}^{-1}$  from 30 to  $200^\circ\text{C}$ . DSC studies were carried out on a Perkin-Elmer Diamond DSC in the temperature range  $40\text{--}220^\circ\text{C}$ , at a heating rate of  $20^\circ\text{C min}^{-1}$  under N<sub>2</sub> flow. All the samples were placed in Al pan and the samples mass in the range of 0.3 to 3.3 mg. For  $\Delta H$  measurements, the DSC system was calibrated with indium ( $m.p.=156.60^\circ\text{C}$ ;  $\Delta H_{\text{fus}}=28.45\text{ J g}^{-1}$ ) and zinc ( $m.p.=419.47^\circ\text{C}$ ;  $\Delta H_{\text{fus}}=108.37\text{ J g}^{-1}$ ).

### Results and discussion

#### FTIR characterization

In order to select the optimal sampling methods, Co, Cu and Zn methanesulfonates are characterized by FTIR using nujol mull difference spectrometry, FTIR-ATR and KBr pellet, respectively. For Co methanesulfonate, the spectra of three methods are similar to each other, and the results are consistent with that of rare earth methanesulfonates [5, 6]. In the case of Cu and Zn methanesulfonates, the absorptions of stretching vibration of  $-\text{SO}_2-$  group using KBr pellet are different from that of the other two methods. Here, IR spectra of Cu methanesulfonate are taken as example for explanation (Fig. 1).

\* Author for correspondence: hjiang78@hotmail.com

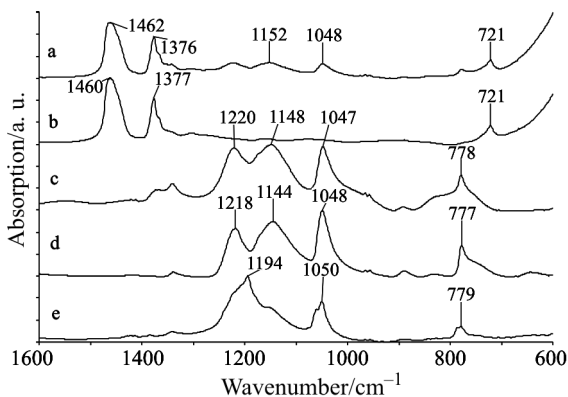


**Fig. 1** IR spectrum of copper methanesulfonate; a – mixture of nujol mull and copper methanesulfonate, b – nujol mull, c – difference spectrum of copper methanesulfonate, i.e. a–b, d – copper methanesulfonate using FTIR-ATR, e – copper methanesulfonate using KBr pellet

Spectrum c in Fig. 1 is the difference spectrum between spectrum a and spectrum b. In spectrum c, the absorption at  $778\text{ cm}^{-1}$  is attributed to the stretching vibration of C–S. The absorption at  $1047\text{ cm}^{-1}$  is attributed to the symmetrical stretching vibration of  $-\text{SO}_2-$  group. Also the absorptions at  $1220$  and  $1148\text{ cm}^{-1}$  are attributed to the asymmetrical stretching vibration of  $-\text{SO}_2-$  group. As can be seen from Fig. 1, the stretching vibration of C–S and symmetrical stretching vibration of  $-\text{SO}_2-$  group are similar to each other of above three methods. Noticeably, the absorptions of asymmetrical stretching vibration of  $-\text{SO}_2-$  group in spectrum c and d show two peaks, while that in spectrum e shows one peak at  $1194\text{ cm}^{-1}$  only. The results demonstrate that solid reactions have taken place possibly during sample preparation by KBr pellet pressing, leading to the change of absorption peak of asymmetrical stretching vibration of  $-\text{SO}_2-$  group.

#### Thermogravimetry and derivative thermogravimetry

The dehydration process of Co and Cu methanesulfonates is investigated in  $\text{N}_2$  atmosphere by TG/DTG at the same heating rate of  $20^\circ\text{C min}^{-1}$  (Figs 2 and 3). The results indicate that they all contain four crystallization water molecules. The calculated values of mass loss of water molecules are in good agreement with the experimental values. As can be seen from TG/DTG curves, dehydration occurs in two steps, and each step corresponds to the liberation of two crystallization water molecules. The dehydration process finishes completely before  $200^\circ\text{C}$ .

In order to determine the effect of different heating rate on the dehydration, four heating rates ( $5$ ,  $10$ ,  $15$  and  $20^\circ\text{C min}^{-1}$ ) are carried out in dynamic  $\text{N}_2$  atmosphere for Zn methanesulfonate (Fig. 4). The calculation results show Zn methanesulfonate contains

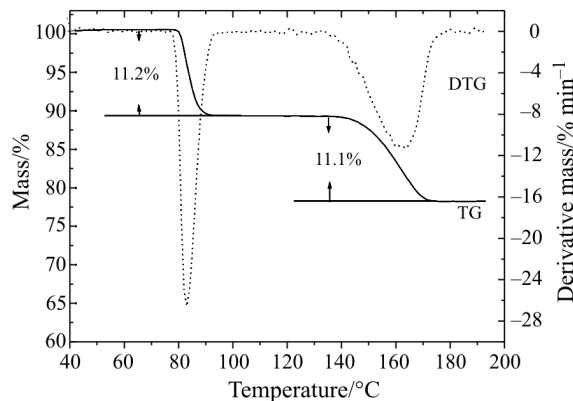


**Fig. 2** TG/DTG curves for  $\text{Co}(\text{CH}_3\text{SO}_3)_2 \cdot 4\text{H}_2\text{O}$

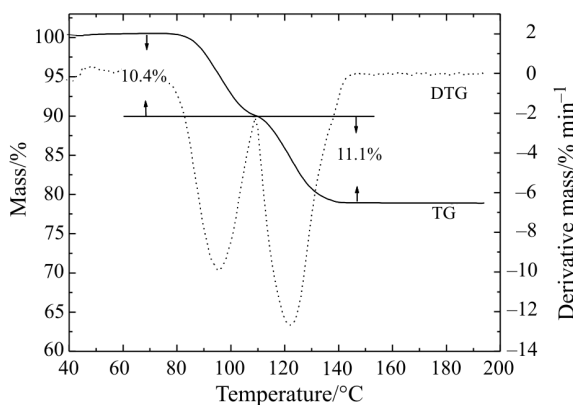


**Fig. 3** TG/DTG curves for  $\text{Cu}(\text{CH}_3\text{SO}_3)_2 \cdot 4\text{H}_2\text{O}$

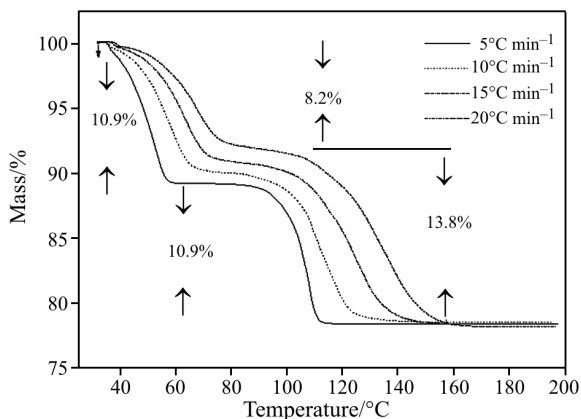


**Fig. 4** TG curves for dehydration of  $\text{Zn}(\text{CH}_3\text{SO}_3)_2 \cdot 4\text{H}_2\text{O}$  at different heating rates

four crystallization water molecules, which dehydrated completely before  $200^\circ\text{C}$ . In the case of  $5^\circ\text{C min}^{-1}$ , each mass loss step of TG corresponds to the elimination of two water molecules. However, in the case of  $20^\circ\text{C min}^{-1}$ , there are 1.3 water molecules liberated followed by the removal of the other remaining 2.7. The peak temperatures  $T_{m1}$  of DTG under four heating rates ( $5$ ,  $10$ ,  $15$  and  $20^\circ\text{C min}^{-1}$ ) are  $324$ ,  $331$ ,  $334$ ,  $338\text{ K}$ , respectively. The peak temperatures

$T_{m2}$  of DTG under four heating rates (5, 10, 15 and  $20^{\circ}\text{C min}^{-1}$ ) are 381, 383, 396, 404 K, respectively. An increase in the heating rate causes an increase in the peak temperature, which means the apparent dehydration temperature becomes higher with the increasing heating rate.

#### Differential scanning calorimetry

The dehydration process of Co, Cu and Zn methanesulfonates is also monitored by DSC in the temperature range of  $40\text{--}220^{\circ}\text{C}$ . Comparing experimental results, we find the endothermic peaks of DSC cannot correspond to the mass loss stages of TG, though TG and DSC measurements are conducted under the same experimental conditions. The same problems also exist in the dehydration of gadolinium and lutetium methanesulfonates [12] and the dehydration of hydrated rare earth *p*-toluenesulfonates [13]. In order to clarify this question, the procedural variables that can affect the experimental results have been investigated. The variables include heating rates, Al pan states (unsealed and sealed), sample mass and sample granularity, etc. In our experiments, methanesulfonates sample are the same size as they are ground in agate mortar before measurements. Therefore, the sample granularity has little effect on the experimental results.

In order to investigate the effect of Al pan state on dehydration, the DSC curves of  $\text{Zn}(\text{CH}_3\text{SO}_3)_2 \cdot 4\text{H}_2\text{O}$  with different sample mass in unsealed and sealed Al pan at the same heating rate are investigated in Fig. 5I and II. As can be observed, the peak temperature of sealed DSC curve is higher than that of unsealed. Meanwhile, the DSC curves of different sample mass under sealed condition do not correspond to the TG/DTG curve, so do Co and Cu methanesulfonates. However, the DSC curves (a and b) of unsealed state seem to be reasonable. Such differences could be explained as follows: in the case of sealed Al pan, the evolved water is not easy to gasify, which may lead to the higher peak temperature of DSC curve. Thus the DSC measurements of Co, Cu and Zn methanesulfonates should be conducted under unsealed condition in the experiments.

The DSC curves of  $\text{Co}(\text{CH}_3\text{SO}_3)_2 \cdot 4\text{H}_2\text{O}$  and  $\text{Cu}(\text{CH}_3\text{SO}_3)_2 \cdot 4\text{H}_2\text{O}$  with different sample mass under unsealed condition are shown in Figs 6 and 7. All DSC curves show two endothermic peaks due to dehydration in two distinct steps, and the second dehydration step needs more heat than the first one (Table 1). Noticeably, the peak temperatures of DSC curves become higher with the increasing sample mass. Such fact suggests a correlation between peak temperature and sample mass. From Table 1, it is evident that the DSC curves of  $0.5\text{--}1.0\text{ mg}$  samples are in good agreement with the TG/DTG curves, while DSC

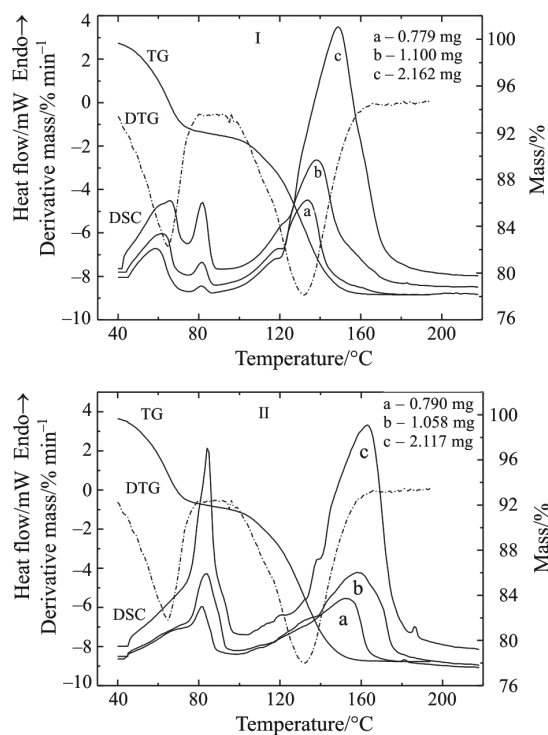


**Fig. 5** TG/DTG/DSC curves of  $\text{Zn}(\text{CH}_3\text{SO}_3)_2 \cdot 4\text{H}_2\text{O}$  with different sample mass in I – unsealed and II – sealed Al pan

curves of more than  $1.0\text{ mg}$  samples lag behind TG/DTG curves. With the sample mass increasing, the decrease of sensitivity probably causes this fact. On the basis of that, we conclude the sample mass of DSC should be in certain proportion to that of TG. In our experiment, the DSC curve of less than  $1.0\text{ mg}$  sample mass show good accordance with TG, and the sample mass of TG is about  $2.5\text{ mg}$ .

The effect of Al pan state and different sample mass on the dehydration at the same heating rate has been discussed above. As can be observed from Fig. 5, the dehydration takes place in two steps using both unsealed and sealed Al pan. But there is a little difference in the first stage. For unsealed one, the DSC curve contains two endothermic peaks, which

**Table 1** Summary for DTG and DSC data of the dehydration process of  $\text{Co}(\text{CH}_3\text{SO}_3)_2 \cdot 4\text{H}_2\text{O}$  and  $\text{Cu}(\text{CH}_3\text{SO}_3)_2 \cdot 4\text{H}_2\text{O}$

<i>M</i>	$T_{m1}/^{\circ}\text{C}$	$T_{m2}/^{\circ}\text{C}$	$m_i/\text{mg}$	$T_1/^{\circ}\text{C}$	$T_2/^{\circ}\text{C}$	$\Delta H_1/\text{J g}^{-1}$	$\Delta H_2/\text{J g}^{-1}$
Co	83.0	164.0	0.368	85.3	156.2	326.9	421.3
			0.761	85.4	163.9	326.4	396.3
			1.305	87.3	171.2	316.6	417.5
			1.847	88.3	180.6	307.0	438.8
Cu	95.3	122.2	0.489	93.6	121.3	279.4	314.6
			1.101	102.3	134.4	297.0	334.0
			2.261	107.6	142.4	316.6	350.8
			3.244	112.6	148.1	318.8	351.4

$m_i$  – sample mass used for DSC measurement;  
 $T_{m1}$ ,  $T_{m2}$  – peak temperature of DTG;  $T_1$ ,  $T_2$  – peak temperature of DSC

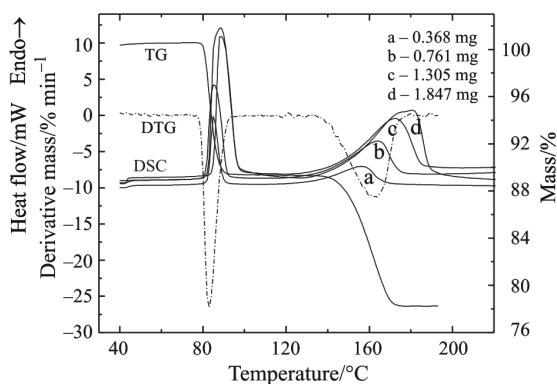


**Fig. 6** TG/DTG/DSC curves of  $\text{Co}(\text{CH}_3\text{SO}_3)_2 \cdot 4\text{H}_2\text{O}$  with different sample mass

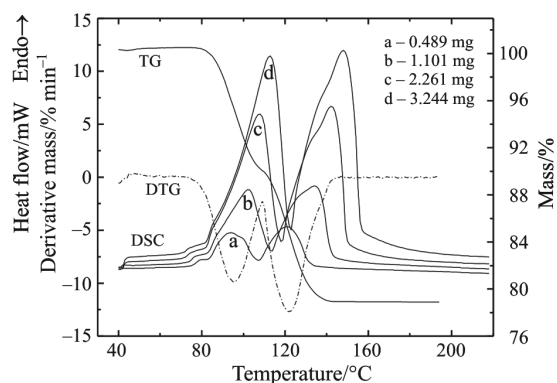


**Fig. 7** TG/DTG/DSC curves of  $\text{Cu}(\text{CH}_3\text{SO}_3)_2 \cdot 4\text{H}_2\text{O}$  with different sample mass

suggest the hydrated salts lose liquid water first and then it transforms into vapor. However, the sealed one only shows one endothermic peak, which means the crystallization water molecules are lost directly in gas state. The experimental results show that the ways of dehydration under unsealed and sealed conditions for zinc methanesulfonate are different below  $100^\circ\text{C}$ .

## Conclusions

- For the IR characterization of copper methanesulfonate, nujol mull difference spectrometry and FTIR-ATR are better than KBr pellet. The solid reactions have taken place probably during sample preparation by KBr pellet pressing, leading to the change of absorption peak of asymmetrical stretching vibration of  $-\text{SO}_2-$  group.

- The dehydration process of  $\text{Co}(\text{II})$ ,  $\text{Cu}(\text{II})$  and  $\text{Zn}(\text{II})$  tetrahydrated methanesulfonates occur in two stages in  $\text{N}_2$  atmosphere. And the temperature of dehydration becomes higher with the increase of the heating rate.
- The DSC measurements of methanesulfonates had better conducted in unsealed Al pan and the sample mass of DSC should be in certain proportion to that of TG. The ways of dehydration under unsealed and sealed conditions for zinc methanesulfonate are different below  $100^\circ\text{C}$ .

## References

- 1 K. Manabe, Y. Mort and S. Kobayashi, *Tetrahedron*, 55 (1999) 11203.
- 2 R. Varala, M. M. Alam and S. R. Adapa, *Synlett*, 1 (2003) 67.
- 3 M. Wang, Z. C. Wang, Z. L. Sun and H. Jiang, *React. Kinet. Catal. Lett.*, 84 (2005) 223.
- 4 K. Ishihara, M. Kubota, H. Kurihara and H. Yamamoto, *J. Org. Chem.*, 61 (1996) 4560.
- 5 E. M. Aricó, L. B. Zinner, C. Apostolidis, E. Dornberger, B. Kanellakopulos and J. Rebizant, *J. Alloys Compd.*, 249 (1997) 111.
- 6 E. M. Aricó, L. B. Zinner, B. Kanellakopulos, E. Dornberger, J. Rebizant and C. Apostolidis, *J. Alloys Compd.*, 323–324 (2001) 39.
- 7 Y. Zhao, B. Sun, Y. Xu, D. Wang, S. Weng, J. Wu, D. Xu and G. Xu, *J. Mol. Struct.*, 560 (2001) 117.
- 8 L. H. Zhang, H. Jiang, H. Gong and Z. L. Sun, *J. Therm. Anal. Cal.*, 79 (2005) 731.
- 9 A. Ramírez, M. L. Gómez and A. Guerrero, *Thermochim. Acta*, 124 (1988) 9.
- 10 K. Egashira, Y. Yoshimura, H. Kanno and Y. Suzuki, *J. Therm. Anal. Cal.*, 71 (2003) 501.
- 11 J. J. Tian, H. Jiang, H. Gong and Z. L. Sun, *J. Therm. Anal. Cal.*, 77 (2004) 825.
- 12 M. F. V. Moura, J. R. Matos and R. F. Farias, *Thermochim. Acta*, 414 (2004) 159.
- 13 A. V. Santos and J. R. Matos, *J. Alloys Compd.*, 344 (2002) 195.

Received: August 8, 2005

Accepted: December 8, 2005

OnlineFirst: May 16, 2006

DOI: 10.1007/s10973-005-7064-2